Photoemission study of the adsorption of Cu on Pt(111)

M. L. Shek, P. M. Stefan,* I. Lindau, and W. E. Spicer
Stanford Electronics Laboratories, Stanford University, Stanford, California 94305
(Received 2 September 1982; revised manuscript received 10 January 1983)

Photoemission experiments have been performed to investigate the electronic structure of Cu adlayers on a Pt(111) surface. The evolution of the 3*d* states as a function of Cu coverage is observed at the Cooper minimum of the Pt 5*d* emission ($h\nu=150$ eV), where the Cu 3*d* emission is enhanced. For Cu coverages up to ~ 0.6 of the first monolayer (ML), the 3*d* states give a symmetrical and resonancelike peak with a maximum at -2.6 to -2.7 eV with respect to the Fermi level E_F, and a full width at half maximum of 1.4 to 0.5 eV. Between ~ 0.6 and ~ 1 ML, there is an increase in Cu 3*d* emission around -3.5 eV, suggesting the onset of two-dimensional delocalization. The delocalization of the 3*d* states increases with increasing Cu coverage. Beyond ~ 1 ML, Cu—Cu bonding states appear below -4 eV as well. The Cu adlayers studied, from submonolayer coverages up to ~ 1.5 ML, show an interesting absence of Cu-derived emission near E_F, in contrast with the flat emission at the corresponding energies shown by pure Cu. For small (≤ 0.6 ML) submonolayer coverage, the Cu $2p_{3/2}$ core level, excited by Mg $K\alpha$ radiation, is observed to be shifted (upward) by -0.60 to -0.65 eV relative to the bulk Cu $2p_{3/2}$ core level. By 3 ML, the Cu $2p_{3/2}$ binding energy is almost identical with that of a pure Cu sample. The adsorption of Cu "removes" the Pt $4f_{7/2}$ surface core level, which then becomes bulklike. The adsorption of Cu also results in a work-function decrease. However, the Pt $4f_{7/2}$ core-level data do not permit the work-function decrease to be explained by simplistic arguments based on charge transfer.

I. INTRODUCTION

There has been much interest in the electronic structures of metal adatoms on metallic as well as nonmetallic surfaces. Among the fundamental problems which are tackled is the evolution of the electronic structures of spatially isolated atoms into the bulk metal. Experimental studies have been made on the adsorption of Cu on *sp* substrates such as[1] Zn and amorphous carbon,[2] which should not interact strongly with the Cu 3*d* states and which provide adsorption sites further apart than the bulk Cu-Cu spacing. It is demonstrated[1,2] that isolated Cu adatoms or a Cu monolayer (ML) have a 3*d* peak binding energy[3] ~ 1 eV larger than that of bulk Cu. The interpretation is that, as the Cu-Cu interatomic separation increases, change in valence 4*s* screening lowers the 3*d* energy levels through Coulombic interactions.[4] The 3*d* peak is also observed to be narrower than the bulk bandwidth, as may be expected from a less delocalized layer. On the other hand, the adsorption of 0.1 ML Cu on Ni(111),[5] a *d*-band substrate, gives a Cu 3*d* peak lying at only 0.35 eV higher binding energy than bulk Cu. It is concluded that, in this case, *d-d* interaction between the adsorbate and the substrate determines the Cu 3*d* peak position.

In this paper, we shall present our photoemission results of Cu adsorption on Pt(111),[6] supplemented by observations using Auger electron spectroscopy and, to a small extent, low-energy electron diffraction. The valence photoemission results will focus on the Cu 3*d* "density of states" in the submonolayer to monolayer regime. A primary motivation is to attempt to extract information on the Pt—Cu bond by observing the Cu adlayer 3*d* states. It then becomes apparent that this requires a knowledge of the adlayer geometric structure, as well as some estimates of the relative contributions of Pt-Cu interaction and Cu-Cu interaction in the presence of the Pt substrate. It is also desirable to look at larger Cu coverages in order to establish trends. We have studied the Cu $2p_{3/2}$ core levels and the work-function changes in the hope that they may be useful in unraveling the complexities of the Pt-Cu electronic interactions.

II. EXPERIMENT

Experiments were performed in a stainless-steel vacuum system described previously.[7] The Pt(111) substrate was typically cleaned by Ar ion sputter and anneal cycles, followed by oxygen heat cleaning.[7] Cu was vacuum-deposited by thermal evapora-

tion from a Cu bead mounted on a resistively heated tungsten wire. The flange onto which the Cu bead assembly was built was equipped with two gold-coated quartz crystals connected to a remote electronic oscillator. One crystal was located below the Cu bead. The other was movable and could be placed in front of the Cu bead. The oscillator indicated the amount of material deposited on each quartz crystal. The relative rates of Cu deposition on the lower and the front crystals were calibrated. The front crystal was then moved away, and the Pt substrate was put in its place for evaporation. During Cu evaporation, the lower crystal monitored the relative amount of Cu deposited on the Pt sample.[8]

The Cu coverage was better calibrated with the use of Auger electron spectroscopy which, in addition, yielded information on the growth mode of the Cu adlayer. The Auger intensities of the Pt substrate and the Cu adsorbate were followed as a function of the relative Cu dosage monitored by the lower quartz crystal (Fig. 1). For a layer-by-layer growth mechanism, the intensities should vary linearly, with a change in slope upon the completion of each layer.[9] The relative Cu dosage at the first break in the slope was noted (t_1). This was the point at which the first saturated monolayer (ML) was formed. The relative Cu dosage could be taken as a function of evaporation time (if the evaporation rate was constant) or as a function of the thickness read by the lower quartz crystal. The Auger intensities of the Cu-covered surface were then measured and related to the relative Cu dosage (t). The ratio of t to t_1 then yielded the Cu coverage on the substrate. Alternately, at the completion of a saturated layer as determined by the Auger intensities, the lower thickness monitor reading was noted (R_1). Then the subsequent determination of the Cu surface coverage was obtained from the ratio of the monitor reading R to the calibration reading R_1, without the further need for measuring the Auger signals. There are two things to be noted here. (1) The Auger calibration and definition of 1 ML works best for Auger electrons with short escape depths; (2) the first completed layer in the Auger calibration only signified the saturation of adsorption sites as governed by the substrate and, possibly, adsorbate-adsorbate interactions. The experimental variations of the values from Auger calibration are typically ± 0.05 ML for submonolayers.

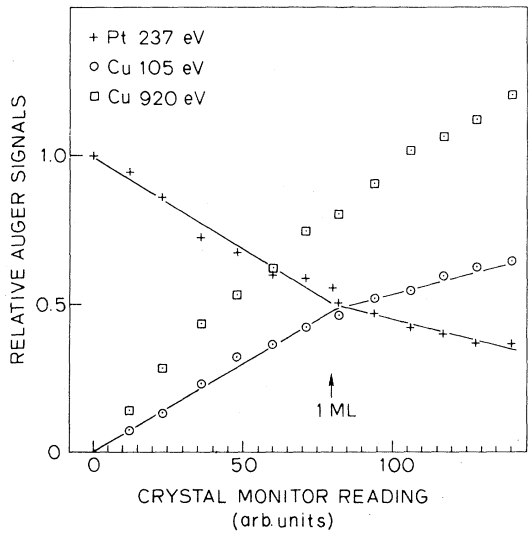

FIG. 1. Auger intensities as a function of relative Cu dosage registered by a thickness monitor. The clean Pt 237-eV Auger signal is normalized to 1.

Surface valence-band structures were studied by means of soft-x-ray photoemission spectroscopy with the use of the 4° beam line at the Stanford Synchrotron Radiation Laboratory.[10,11] We shall report the results on the Cu $3d$ states, obtained at a photon energy of 150 eV, where the Pt $5d$ emission is suppressed owing to the Cooper minimum. The results at other photon energies are given elsewhere.[7] The Cu $2p_{3/2}$ core level was studied by x-ray photoemission spectroscopy with the use of a Mg $K\alpha$ source, providing a photon energy of 1253.6 eV. Photoelectrons were collected by a double-pass cylindrical mirror analyzer. The total instrumental resolution for the valence spectra was about 0.5 eV. For the core-level spectra, the total resolution was 0.8 eV. The change in work function induced by Cu adsorption was obtained from the change in the width of the photoelectron energy distribution excited by $h\nu$ of 150 eV.

III. RESULTS

A. Auger-electron-spectroscopy and low-energy electron-diffraction observations

Figure 1 shows the variations of the Pt 237 eV Auger intensity as well as the Cu 105 and Cu 920 eV Auger intensities, as a function of relative Cu deposition registered by the lower quartz crystal. The data are for room-temperature adsorption. For the purpose of this plot, the absolute reading of the lower crystal monitor is immaterial as long as it denotes a linear variation of the real surface coverage. It is seen that the initial variations of the Auger intensities are approximately linear with respect to the amount of Cu deposited. Breaks in the slopes occur, however, at about 84 (80 to 88) for the Pt 237-eV curve, and about 80 (78 to 82) for the Cu 105-eV curve. Then the curves continue to decrease or increase with different slopes. As expect-

ed, the change in slope of the Cu 920-eV curve, upon the completion of the first saturated layer, is not as sensitive as the other curves.

Low-energy electron diffraction shows that Cu adlayers (0.27, 0.55, 0.83, and 1.08 ML) do not induce any superlattice structures. There is a sharp (1×1) pattern. However, it is noticed that, even for about 0.27 ML Cu adsorbed at room temperature, distinct changes have occurred in the diffracted beam intensities. For instance, at a primary beam voltage of 147 V and an angle of incidence of about 5°, the (0,0) diffracted beam of clean Pt(111) is indistinguishable from the background. Under the same observation conditions, however, the presence of even 0.27 ML Cu leads to a greatly enchanced intensity of the (0,0) diffracted beam. Therefore Cu adsorption is likely to proceed epitaxially as will be discussed later.

B. Photoemission data on Cu 3*d* states of Cu on Pt(111)

Figure 2 shows the valence photoemission spectra of several Cu coverages on Pt(111) at room temperature. The conspicuous feature in each spectrum is the Cu 3*d* peak with a maximum around -2.6 eV relative to the Fermi level. This is identified as Cu 3*d*-derived owing to the photon-energy dependence of the valence-band features.[7] At the lowest coverage [curve (1)], the shoulder at -0.4 eV is due to the Pt substrate, as are the hints of some structures around -4 and -6 eV. In the other curves, the Pt contribution is negligible. It is seen that, as the Cu coverage increases, the 3*d* states become broadened and asymmetric. At ~10 ML [curve (5)], shoulders are apparent around -3.5 and -4.5 eV. At this point, the overlayer should well approximate bulk Cu, and the onset of the *d*-band emission becomes sharper compared with that of a rather well localized adlayer [curves (3) or (4)]. There is also a small increase in emission below and at the Fermi level.

The evolution of the 3*d* peak shape from 0.075 ± 0.025 ML to approximately 1.5 ML is shown in Fig. 3 as successive difference curves $\Delta'N(E)$. These successive difference curves are obtained by subtracting, from each spectrum, the spectrum corresponding to the preceding lower Cu coverage.[12] The lack of systematic changes in the successive difference curves $\Delta'N(E)$ up to 0.64 ± 0.03 ML [curves (1) to (5)] means that each addition of Cu preserves the same 3*d* peak shape. However, the next addition of 0.1 ML shifts the centroid of the increased 3*d* states by 0.3 to 0.4 eV (downward) to

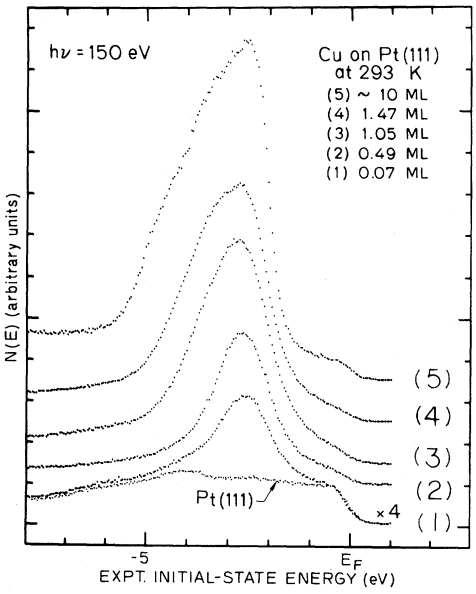

FIG. 2. Photoelectron energy distributions $N(E)$ at $h\nu=150$ eV of several surface coverages of Cu on Pt(111) at room temperature. (1) 0.075 ML, magnified by a factor of 4. (2) 0.495 ML. (3) 1.05 ML. (4) 1.47 ML. Curve (5) is a ~10 ML thick overlayer.

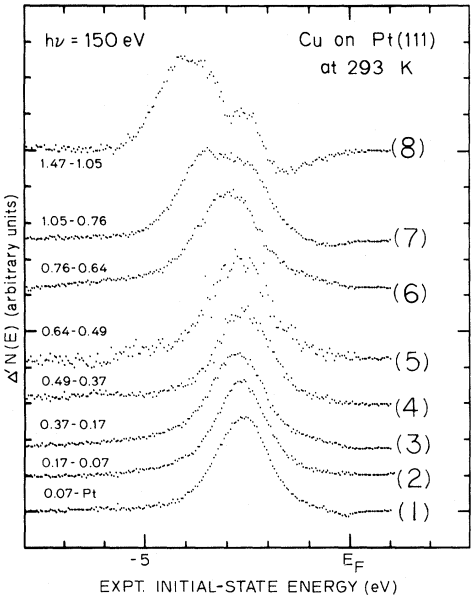

FIG. 3. Successive difference curves $\Delta'N(E)$ between the valence spectra of various Cu-covered Pt(111) surfaces at room temperature. $h\nu=150$ eV. The peak heights are approximately normalized to one another. (1) 0.075 ML—clean Pt(111). (2) 0.17—0.075 ML. (3) 0.37—0.17 ML. (4) 0.495—0.37 ML. (5) 0.64—0.495 ML. (6) 0.765—0.64 ML. (7) 1.05—0.765 ML. (8) 1.47—1.05 ML.

-3.0 eV [curve (6)]. Between 1.05 ± 0.05 and 0.76 ± 0.05 ML [curve (7)], the change consists of not only a further increase in $3d$ states around -2.6 eV but also a new feature around -3.5 eV. The addition of Cu beyond 1 ML leads to the appearance of new $3d$ states with binding energies greater than -4.1 eV. A small negative change at about -1.5 eV also appears, reflecting a sharper rise of the Cu $3d$ peak on the low binding energy side as the Cu coverage increases.

Figure 4 shows the successive difference curves for the adsorption of Cu on Pt(111) at 160 K. The behavior is largely similar to that at room temperature. A small difference exists: Between 1 and 0.8 ML [curve (7)], there is some structure below -4.0 eV, which is absent for room-temperature adsorption. However, such a difference may arise from the experimental error associated with the Cu coverage, and therefore should not be attributed to the different temperatures of adsorption without further experimental support. In agreement with the results at room temperature, Fig. 4 shows that the Cu $3d$ peak shape starts to broaden and become asymmetric [curve (5)] after about 0.6 ML.

To further explore the factors governing the Cu $3d$ peak shape, Fig. 5 gives a comparison between

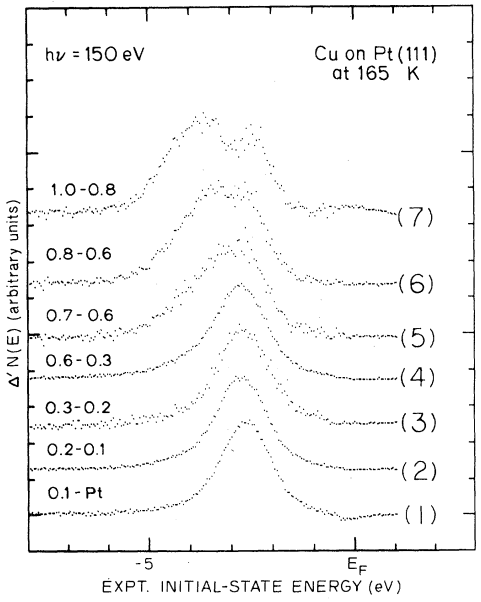

FIG. 4. Successive difference curves $\Delta' N(E)$ between the valence spectra of various Cu-covered Pt(111) surfaces at 165 K, $h\nu=150$ eV. The peak heights are approximately normalized to one another. Curve (1) 0.1 ML—clean Pt(111). (2) 0.2—0.1 ML. (3) 0.3—0.2 ML. (4) 0.6—0.3 ML. (5) 0.7—0.6 ML. (6) 0.8—0.6 ML. (7) 1—0.8 ML.

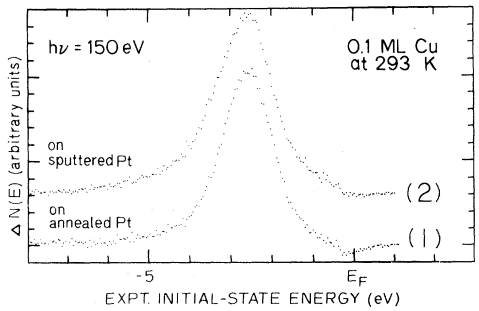

FIG. 5. Comparison between the $\Delta N(E)$ of 0.1 ML Cu on annealed Pt(111) and 0.1 ML Cu on sputtered Pt(111). These are difference curves with reference to the Pt substrate. $h\nu=150$ eV.

the adsorption of about 0.1 ML Cu on a sputtered Pt(111) surface and on the annealed surface. The residual carbon on the sputtered surface may be estimated to be $\gtrsim 20\%$. It is seen that, on the sputtered surface [curve (2)], the Cu $3d$ peak is also located at -2.6 eV. However, there seems to be a shoulder around -3.4 eV and the full width at half maximum (FWHM) is 1.65 to 1.70 eV, slightly larger than the FWHM of 1.5 eV for the Cu on the annealed surface[13] [curve (1)].

C. Photoemission data on core levels

Figure 6 shows the Cu $2p_{3/2}$ core level of various coverages of Cu on Pt(111) at room temperature. The $2p_{3/2}$ spectrum of a Cu(110) sample is also shown. At 0.3 ML Cu, the lowest coverage for which data were taken [curve (1)], the $2p_{3/2}$ binding energy is upward shifted by -0.60 to -0.65 eV relative to the Cu(110) $2p_{3/2}$ binding energy [curve (6)]. Up to 0.6 ML [curve (2)], the peak maximum remains the same as that of 0.3 ML. By 0.9 ML [curve (3)], the magnitude of the shift has decreased to between -0.45 and -0.50 eV. The change between 0.9 and 2 ML is approximately 0.4 eV. At about 3 ML [curve (5)], the peak maximum is essentially the same as that of Cu(110) $2p_{3/2}$. The FWHM for all the spectra is 1.4 to 1.5 eV.

The Pt $4f_{7/2}$ core level after the adsorption of 1 ML Cu has also been observed, with a photon energy of 150 eV. The data are presented in Fig. 7. In Fig. 7(a), we note that the low-binding-energy edge of the Cu-covered Pt $4f_{7/2}$ spectrum in curve (2) is shifted by approximately 0.2 eV towards higher binding energy relative to the rising edge of the clean Pt $4f_{7/2}$ spectrum in curve (1). There are no new structures observed in the Pt $4f_{7/2}$ spectrum. In Fig. 7(b), we show that the Pt $4f_{7/2}$ spectrum in the presence of 1 ML Cu consists of a single peak that can be fitted with a Doniach-Sunjic line

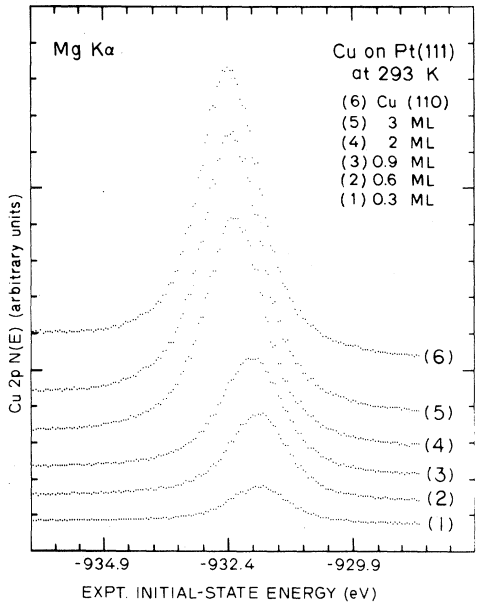

FIG. 6. The Cu $2p_{3/2}$ photoelectron energy distributions $N(E)$ of various Cu coverages on Pt(111) at room temperature. Excited by Mg $K\alpha$, $h\nu=1253.6$ eV. (1) 0.3 ML. (2) 0.6 ML. (3) 0.9 ML. (4) 2 ML. (5) 3 ML. (6) Pure Cu(110) sample, with Cu $2p_{3/2}$ peak maximum at -932.4 eV.

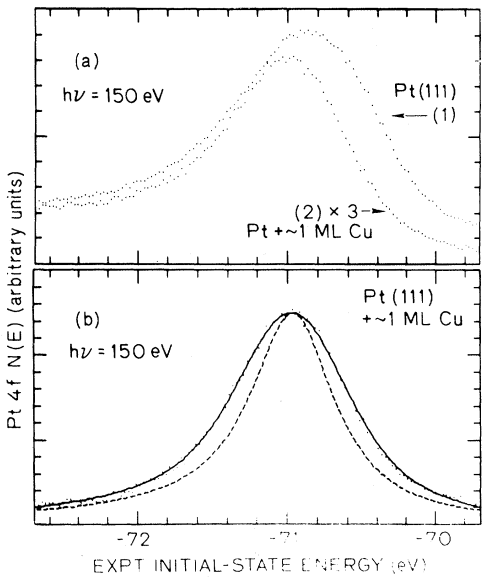

FIG. 7. Effect of Cu on the Pt $4f_{7/2}$ spectrum, $h\nu=150$ eV. (a) Data prior to background subtraction. (1) Clean Pt(111) $4f_{7/2}$ spectrum. (2) Pt $4f_{7/2}$ spectrum after adsorption of 1.05 ML Cu, magnified by a factor of 3.0. (b) Result of fitting Pt $4f_{7/2}$ of (Pt + 1.05 ML Cu) with Doniach-Sunjic line shape. The dotted line (· · · ·) denotes data after background subtraction; the dashed line (— — —) denotes core level with peak maximum at -70.9 eV, natural linewidth 0.66 eV and asymmetry parameter 0.05; the solid line (——) denotes the convolution of the core level with a Gaussian of FWHM 0.35 eV.

shape.[14] The peak maximum lies at -70.9 ± 0.06 eV. The natural FWHM is 0.66 eV, and the asymmetry parameter is 0.05. The Doniach-Sunjic lineshape fit is discussed in a related paper, which also shows that the clean Pt(111) $4f_{7/2}$ spectrum consists of two components. The major component is similar to the Pt $4f_{7/2}$ core level shown in Fig. 7(b), while there exists a smaller component with a peak maximum shifted by ~ -0.4 eV, towards smaller binding energy (towards the Fermi level). The smaller component is the surface core level, and its removal by the Cu monolayer will be discussed in Sec. IV E.

D. Work-function variation

Figure 8 shows the work-function variation as a function of Cu coverage. The variation is nonlinear even for the smallest submonolayers. As the Cu coverage increases, each Cu atom added leads to a smaller change in work function. The work function decreases monotonically from the clean Pt(111) value of 5.5 eV. The work-function change is -1.26 ± 0.06 eV by 1 ML. For comparison, the work functions of pure Cu range from 4.94 to 4.48 eV for the (111) and (110) faces, respectively.[15]

IV. INTERPRETATION AND DISCUSSION

A. Geometric structure of Cu submonolayer on Pt(111): interpretation of results

Our Auger data are consistent with a model of two-dimensional adsorption of Cu on Pt(111) at room temperature, with a coverage-independent

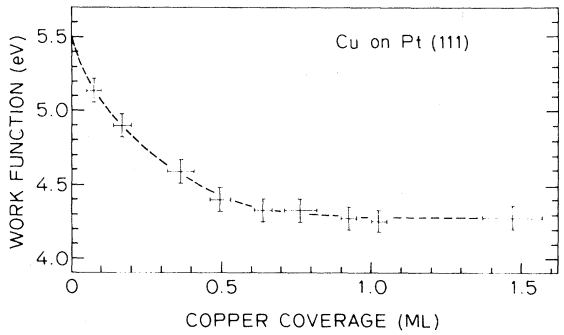

FIG. 8. Work function as a function of Cu coverage on Pt(111) at room temperature. This set of data were derived from the low-energy cutoff (not shown) corresponding to the photoelectron energy distributions in Fig. 2.

sticking coefficient. Two-dimensional growth may be expected because the Pt—Cu bond is stronger than the Cu—Cu bond. Further, the lower surface energy of Cu, compared with the surface energy of Pt, favors the spread of the Cu adatoms on the Pt surface if the interfacial energy is small compared with the difference in surface energies.[16] Both are crude statements based on the assumption that no drastic modifications of the Cu-adatom electronic structures occur upon adsorption on the Pt surface. The coverage-independent sticking coefficient, and the finding that Cu does not adsorb on other Cu adatoms until the first layer is completed, indicates that the Cu atoms have a high mobility on the surface before it becomes adsorbed in an energetically favorable site.

The low background intensity in our low-energy electron diffraction LEED observations suggests that the Cu adlayer is not disordered. The sharp (1×1) pattern, with definite changes in the diffracted beam intensities, indicate that the Cu submonolayers are epitaxial. This is consistent with the observation of ordered CO chemisorbed layers on these Cu adlayers.[17] The Cu adatoms are thus separated from one another by the Pt-Pt interatomic distance of 2.77 Å. The detailed geometric structure of the Cu adlayers should be investigated in future work.

B. Comparison with other work on Cu adsorbed on Pt

The underpotential electrodeposition of Cu on a Pt(111) electrode shows that the Cu atoms first bind to the Pt surface with adsorption energies which are substantially larger than the adsorption energy of Cu on Cu.[18] However, it is reported that Cu deposition on Cu commences when only $\frac{2}{3}$ of the Pt surface atoms are covered. This is in disagreement with our interpretation given in the last section.

A previous study on the Cu $2p_{3/2}$ core level[19] of vacuum-deposited Cu on polycrystalline Pt has revealed a larger shift (−0.95 eV) compared with our value (−0.65 to −0.6 eV). For submonolayer coverages greater than $\frac{1}{10}$ of the Pt surface atoms, a gradual approach towards the bulk Cu $2p_{3/2}$ binding energy is attributed to the presence of Cu clusters.[19] However, it is difficult to reconcile our results with data obtained on polycrystalline samples and with a different Cu coverage calibration.

C. Cu 3*d* peak shape

The evolution of the Cu 3*d* states on Pt(111) reflects three stages: (1) Below approximately 0.6 ML there is a narrow (FWHM 1.5 eV) and rather symmetric peak, due to islands of Cu adatoms located at Pt-Pt spacing. (2) Between 0.6 and 1 ML, with increasing Cu-Cu lateral interaction in the adlayer, bonding states appear at about −3.5 eV. (3) Beyond 1 ML, Cu—Cu bonding interlayer interaction leads to the appearance of bonding states below −4 eV as well.

On the sputtered surface, the larger width and the small asymmetry in the Cu peak shape is probably due to the formation of clusters even at 0.1 ML Cu. The irregularity of the surface provides sites which allow for close Cu-Cu contact. These sites are probably associated with highly uncoordinated Pt surface atoms or carbon impurities. On the other hand, the increased lateral Cu-Cu interaction commencing after 0.6 ML on a smooth surface is likely to arise from an increasing number of Cu atoms in nearest-neighbor sites, leading to a greater delocalization of the 3*d* electrons. In any case, both these two situations contrast with the narrow and symmetric peak below 0.6 ML. This lends support to our interpretation (in Sec. IV A) that the Cu interatomic spacing within the two-dimensional adlayer is probably the same as Pt-Pt spacing. Thus the effects of Pt—Cu bonding should dominate over Cu-Cu lateral interactions in this low-coverage regime.

The Cu 3*d* feature around −3.5 eV in the monolayer may be explained as follows. If one thinks of the Cu adatom *d* orbitals to be oriented as the *d* orbitals of a Cu atom in a (111)-oriented layer, then the *xy*, *yz*, and *zx* orbitals are directed towards the nearest-neighbor Cu atoms in the adlayer. As the Cu coverage increases, these orbitals interact strongly enough to form bonding states within the adlayer. We note that the −3.5-eV feature observed for pure Cu, in this work and in other reports as well,[20,21] lies at a peak in the t_{2g} projected density of states.[21] In particular, this peak is likely to arise from Γ'_{25} and L_3 in the Brillouin zone.[20,22] At this energy, the e_g projected density of states is quite significant, though it contributes to a smaller extent.[21,23] However, the e_g orbitals in the monolayer, the $(x^2\text{-}y^2)$ and $(3z^2\text{-}r^2)$ orbitals, are not directed towards any next-nearest Cu neighbors as in the bulk. Therefore, they should contribute little to the bonding within the adlayer.

For a Cu monolayer on[5] Ni(111) and on Zn(0001),[1] considerable asymmetry has been observed in the Cu subband of the valence spectra excited by He I. A Cu overlayer on Ni(111) is calculated to have a peak in the density of states at about 1 eV below the main *d* peak, and a Cu monolayer on Zn(0001) is calculated to have a structure at about 0.75 to 0.8 eV below the main *d* peak. However, in these reports no structure below the *d* peak maximum is identified, with an experimental resolution which should be better than 0.3 to 0.4 eV.

The further broadening of the $3d$ states beyond 1 ML Cu on Pt(111), with the eventual formation of the -4.5-eV states, are expected as Cu 3d-3d bonding increases. However, the sharper onset of the $3d$ band in the thick Cu overlayer deserves some comments. This may be visualized as a decrease in emission around -1.5 eV and an increase in states near the d-band maximum, moving the peak maximum slightly towards the Fermi level. A similar effect has been observed for Cu on polycrystalline Ag.[24] The sharper d-band onset is a consequence of three-dimensional delocalization. We note that several theoretical studies predict that coupling a Cu monolayer to the underlying layers tend to move the d-band rising edge towards higher binding energy.[23,25] By no means do our data bear on such an expectation.

D. Interpretation of experimental binding energies with the use of a thermodynamical model

In this section, we shall attempt to put into some perspective the binding energies measured for the Cu adatoms. For a plausible interpretation of the observed binding energies, we shall make use of the thermodynamical model proposed by Johansson and Mårtensson.[26] This model incorporates the effects of final-state relaxation. It has been quite successful in estimating surface core-level shifts[27] and alloy core-level shifts.[28,29] Then the binding energy (with respect to the Fermi level) of level l of the adatom on the metal B is

$$E_l^{Z\text{ on }B}=E(Z\text{ on }B)+\epsilon_l-E(Z+1\text{ on }B)\ , \tag{1}$$

where Z is the atomic number of the adatom, $E(Z\text{ on }B)$ is the heat of adsorption of the Z atom on B, taken to be positive, and ϵ_l is the energy required to excite the electron from level l of the Z atom to the least-bound valence orbital of the $(Z+1)$ atom.[26,30]

We would like to compare $E_l^{Z\text{ on }B}$ with the observed binding energy of level l in bulk Z metal, which is[26]

$$E_l^{Z\text{ bulk}}=E_{\text{coh}}^{Z}+\epsilon_l-E_{\text{coh}}^{Z+1}-E(Z+1\text{ in }Z)\ . \tag{2}$$

In Eq. (2), E_{coh}^{Z} and E_{coh}^{Z+1} are the cohesive energies of the Z and $(Z+1)$ metals, respectively. $E(Z+1\text{ in }Z)$ is the differential heat of solution of the $(Z+1)$ metal in the Z metal, and we take it to be positive for an exothermic solution process. We note that the quantity $(E_l^{Z\text{ on }B}-E_l^{Z\text{ bulk}})$ is independent of ϵ_l.

For heats of adsorption and solution, it is convenient to use the values calculated by Miedema's semiempirical method.[31–33] Therefore, the values for E(Cu on Pt), E(Zn on Pt), and E(Zn in Cu) are 3.315, 2.331, and 0.3089 eV per atom, respectively. The cohesive energies for Cu and Zn are 3.5 and 1.35 eV per atom, respectively.[34] With the use of these values and Eqs. (1) and (2), it is estimated that the core level of Cu on Pt is shifted by -0.86 eV (upward) relative to the core level of Cu in bulk Cu.

In our experiment, the kinetic energy of the Cu $2p_{3/2}$ photoelectron is around 3.15 eV, which yields a surface sensitivity of 6 to 7.5 Å after correction for the geometry of detection. The surface layer contribution is estimated to be 0.20 to 0.34 of the signal from pure Cu,[35] and the observed Cu $2p_{3/2}$ binding energy is a good approximation to the bulk Cu $2p_{3/2}$ binding energy.[36] The experimentally observed shift of Cu $2p_{3/2}$ on Pt(111), relative to the approximate bulk Cu $2p_{3/2}$ binding energy, is -0.60 to -0.65 eV (upward) at about 0.3 ML coverage. This is in fair agreement with the crude estimate of -0.86 eV for an isolated Cu adatom. The small difference may be due to the presence of lateral Cu-Cu interaction in the adlayer. Since the shift of a Cu atom in the surface of Cu can be estimated to be -0.37 eV, the effect of Cu-Cu lateral interaction in the adlayer is to offset the shift experienced by an isolated Cu adatom. It is also apparent that part of the upward shift observed for Cu $2p_{3/2}$ on Pt is a surface effect: The adatom electronic structure and final-state relaxation differ from those in bulk Cu by virtue of its location on a surface.

When the same scheme is applied to the centroid of the Cu $3d$ states, ϵ_l in Eqs. (1) and (2) may be crudely approximated[37,38] by the atomic excitation energy of $d^{10}s\rightarrow d^9s^2$. If ϵ_l is taken to be 1.489 eV, which is the weighted average over excitation to the spin-orbit multiplets[39] of d^9s^2, the centroid of the $3d$ states in bulk Cu can be estimated to be -3.33 eV.[40] However, for the purpose of comparison between Cu atoms in different environments, the value of ϵ_l is again immaterial.

The experimental binding energies obtained in our valence-band spectra contain greater ambiguities than the core-level binding energies presented so far. In the pure Cu valence spectrum [curve (5) in Fig. 2], the contribution of the surface layer is estimated to be 0.5 of the total signal.[35] Since the second-layer electronic density of states is already bulklike,[23] the observed centroid around -3.1 eV may be intermediate between the surface $3d$ centroid and the bulk $3d$ centroid and the bulk $3d$ centroid. In view of these uncertainties, we make use of the x-ray photoemission spectrum of Cu $3d$,[20] which yields a centroid energy -3.2 to -3.3 eV. Hence the use of

Eqs. (1) and (2), with an atomic excitation energy for E_I, has given quite a good estimate of the $3d$ centroid. The experimental Pt-Cu $3d$ centroid shift is ~ -0.60 eV relative to bulk Cu.

It should be noted that, according to this scheme, the Cu valence $3d$ centroid and Cu core $2p$ level undergo the same energy shift relative to pure bulk Cu. As shown above, the experiment indeed shows such a correlation. The results given in the above discussion are listed in Table I. In order to see how general the above results are, we have also listed the results for Cu in other environments. In the table, two calculated sets of values are given. Those under the columns labeled (1) are based on the heats of solution estimated from Miedema's method alone.[31–33,41] The calculated values under the columns labeled (2) have incorporated the experimental heats of solution which are available.[42,43] These two calculated sets of values are quite similar. There is a general agreement between the calculated and the observed values for the $3d$ centroids, possibly except for the case of Cu in Ni.[44] The calculated surface-binding-energy shift of pure Cu, relative to the pure bulk, is surprisingly close to the shift (-0.36 eV) given by a first-principles calculation for the $3s$ orbital of Cu(100),[45] as well as the experimental value (-0.25 eV).[46] The correlation between the $3d$ centroid shift and the $2p$ core-level shift, noted previously for Cu on Pt(111), also exists for other Pt-Cu systems[7] and for Cu in Zn.[47] In spite of the simplicity of the calculation, it reproduces the trend in the Cu $2p$ energy shifts observed for the Cu species in various environments.

The model used does not permit an analysis of binding energies in terms of electronic interactions. In particular, it does not address the possibility that the Cu component may have an "atomiclike" electron configuration which is sufficiently different from the bulk Cu electron configuration $3d^{9.6}4s^{1.4}(4p)$,[48] so as to cause energy shifts via intra-atomic Coulomb and exchange interactions. However, it is apparent that final-state relaxation can play an important role in determining the observed binding-energy shifts relative to the bulk binding energy. The importance of final-state relaxation in determining such energy shifts, in both valence and core-level photoemission, has been demonstrated theoretically.[45,48]

E. Pt $4f$ core-level and work-function change

Elsewhere,[17] we show that the clean Pt $4f_{7/2}$ core spectrum consists of a bulk core level and a surface core level. The surface core level has a binding-energy shift of approximately -0.4 eV relative to the bulklike core level. In the presence of a monolayer of Cu, the surface core level becomes bulklike, as indicated by the movement of the lower binding-energy edge of Pt $4f_{7/2}$ towards higher binding energy. Thus there is only a single type of Pt core level [Fig. 7(b)].

The above result precludes the interpretation of

TABLE I. Binding energies of various Cu $3d$ centroids and Cu $2p_{3/2}$ core levels relative to bulk Cu. The calculated values are derived using Eqs. (1)–(3), based on the thermodynamical model of Johansson and Mårtensson (Ref. 26). The $3d$ centroids are calculated with an atomic excitation energy ϵ_I of 1.489 eV for Cu $3d^{10}4s^1 \rightarrow 3d^9 4s^2$ (Refs. 37 and 39). The columns labeled (1) are based entirely on energy values calculated from Miedema's semiempirical method (Refs. 31, 32, and 41). The columns labeled (2) incorporate experimental energy values which are available (Refs. 42 and 43).

Environment of Cu	Calculated (eV) 3d centroid (1)	3d centroid (2)	Energy shift (1)	Energy shift (2)	Observed (eV) Cu 3d shift	Cu 2p shift
In bulk	3.33	3.40	0	0	0[a]	0
At Cu surface	2.96	3.01	−0.37	−0.38		−0.25[e]
Adatom on Cu	2.68		−0.65			
In bulk Pt	2.50	2.59	−0.83	−0.81	(−0.7)[b]	(−0.82)[b]
At Pt surface	2.24	2.32	−1.09	−1.08	(−1.0)[b]	(−1.0)[b]
Adatom on Pt	2.47		−0.86		−0.60	−0.62
In bulk Ni	2.73	2.84	−0.60	−0.56	+0.15[c]	−0.32
In bulk Zn	3.92	4.03	+0.59	+0.63	+0.75[d]	0.4[d]

[a] Reference 20.
[b] These values consist of both surface and bulk contributions. See Ref. 7.
[c] Reference 44.
[d] Reference 47.
[e] Reference 46.

the Cu-induced work-function decrease in terms of electron transfer from Cu to the Pt substrate. Instead, the observed work-function decrease has to be attributed to other possibilities which are not mutually exclusive: (1) There may be a polarization of the Cu valence electrons, especially the loosely bound 4*s* electron, towards the Pt substrate. (2) The surface dipole at the Cu adlayer-vacuum interface is different from the surface dipole at the clean Pt-vacuum interface.

V. SUMMARY

We have utilized the Cooper minimum in the Pt 5*d* photoionization cross section ($h\nu = 150$ eV) to observe the evolution of the 3*d* states of Cu adlayers on Pt(111). The 3*d* states vary with Cu coverage in the following manner. (1) Below ~ 0.6 of the first monolayer (ML), the Cu 3*d* states are relatively localized, giving rise to a symmetrical and resonance-like peak with a maximum at -2.6 to -2.7 eV with respect to the Fermi level, and a full width at half maximum of ~ 1.5 eV. In this low-coverage regime, the Cu adlayers are epitaxial and direct Pt-Cu interactions are dominant. No significant Cu-Cu direct interactions are apparent. (2) Between ~ 0.6 and 1 ML, intralayer Cu—Cu bonding leads to an increase in Cu 3*d* states around -3.5 eV. (3) Beyond 1 ML interlayer Cu—Cu bonding states appear below -4 eV as well.

The shift of ~ -0.6 eV (upward) of the adlayer Cu 3*d* states, relative to the centroid of bulk Cu 3*d* states, is very similar to the shift of the adlayer Cu $2p_{3/2}$ core level with respect to the bulk Cu $2p_{3/2}$ core level. Such a correlation between the Cu valence- and core-electron binding energies also exists for other Pt-Cu systems.

On the other hand, the adsorption of 1 ML Cu on Pt(111) only reverts the Pt $4f_{7/2}$ surface core level to the bulklike core level, without introducing any new structure in the $4f_{7/2}$ spectrum. This suggests that the Cu $2p_{3/2}$ core-level shift of -0.6 to -0.65 eV is not due to any electron transfer. Instead, the Cu $2p_{3/2}$ core-level shift arises either from electron rearrangement within the Cu constituent, or from a change (an increase) in final-state relaxation energy. These two effects are not mutually exclusive. Moreover, this upward shift in the Cu core level may not be entirely due to the presence of the Pt substrate, but may be due in part to a surface-versus-bulk core-level shift.

The adsorption of Cu is observed to decrease the work function, which changes from 5.5 eV for the clean Pt(111) sample to ~ 4.3 eV upon the evaporation of $\gtrsim 1$ ML Cu on Pt(111). Any interpretation in terms of electron transfer from Cu to Pt would be inconsistent with the Pt $4f_{7/2}$ core-level data. We hope that these results and our tentative discussion will be substantiated by further work.

ACKNOWLEDGMENTS

We wish to thank R. Morris for his technical assistance and C. Binns for his help in some of our experiments. One of us (W.E.S.) would like to acknowledge J. H. Sinfelt for an interesting discussion. We acknowledge V. S. Sundaram and G. G. Kleiman, and Conselho Nacional de Pesquisas (CNPQ) (Brazil). This work was supported in part by National Science Foundation Grant No. INT-78-07268. The experiments were performed at the Stanford Synchrotron Radiation Laboratory, which is supported by the National Science Foundation through the Division of Materials Research.

---

*Present address: National Laboratory for High-Energy Physics, Oho-machi, Tsukuba-gun, Ibaraki-ken 305, Japan.

[1]I. Abbati, L. Braicovich, C. M. Bertoni, C. Calandra, and F. Manghi, Phys. Rev. Lett. 40, 469 (1978).

[2]W. F. Egelhoff and G. G. Tibbetts, Phys. Rev. B 19, 5028 (1979).

[3]By "binding energy," we mean the absolute magnitude of the observed energy difference between the Fermi level and the electronic energy level in question. Later on, experimental (expt.) initial-state energy denotes the observed energy of the electronic level with reference to the Fermi level, the Fermi level being defined as energy zero.

[4]L. Hodges, R. E. Watson, and H. Ehrenreich, Phys. Rev. B 5, 3953 (1972).

[5]I. Abbati, L. Braicovich, A. Fasana, C. M. Bertoni, F. Manghi, and C. Calandra, Phys. Rev. B 23, 6448 (1981).

[6]In the earliest stage of our work on PtCu systems, when the extent of Cu surface segregation in PtCu alloys was not known to us, Cu evaporation on Pt was first done to simulate an extreme case of Cu segregation to the surface.

[7]M. L. Shek, P. M. Stefan, I. Lindau, and W. E. Spicer, following paper, Phys. Rev. B 27, 7288 (1983). The 3*d* centroid of a diffusion-formed PtCu(111) surface with dilute Cu concentration is at -2.55 eV; the bulk contributes $\sim 50\%$ to the observed 3*d* signal. The 3*d* centroid of a PtCu(110) surface showing Cu segregation is

at −2.25 eV; the bulk contributes ~17% to the signal if the change in Cu concentration is confined to the topmost surface layer.

[8]The thickness monitors could provide a rough estimate of the Cu coverage, if a certain thickness could be identified for one atomic layer. In the course of experiments, this thickness was taken to be 2.55 Å. The value 2.55 Å is the diameter of a Cu atom in bulk Cu. However, the choice of a thickness for an atomic layer contained some arbitrariness, since the interplanar spacing of Cu(111) is 1.8 Å. Moreover, the Pt substrate might not be in exactly the same position as the front quartz crystal to receive the same flux of Cu atoms.

[9]D. C. Jackson, T. E. Gallon, and A. Chambers, Surf. Sci. 36, 381 (1973).

[10]F. C. Brown, R. Z. Bachrach, and N. Lien, Nucl. Instrum. Methods 152, 73 (1978).

[11]I. Lindau and W. E. Spicer, in *Photoemission as a Tool to Study Solids and Surfaces,* Chap. 6 in *Stanford Synchrotron Radiation Research,* edited by S. Doniach and H. Winick (Plenum, New York, 1980).

[12]The inelastic background is first subtracted from the valence-band spectra before the difference curves are taken. The subtraction is done by assuming a linear-scattered background between the bottom of the valence band and the Fermi level.

[13]1.4 eV if corrected for the experimental energy resolution. Unless otherwise stated, the reported values are the observed values without correction.

[14]S. Doniach and M. Sunjic, J. Phys. C 3, 285 (1970).

[15]P. O. Gartland, S. Berge, and B. J. Slagsvold, Phys. Norv. 7, 39 (1973).

[16]E. Bauer and H. Poppa, Thin Solid Films 12, 167 (1972).

[17](a) M. L. Shek, P. M. Stefan, I. Lindau, and W. E. Spicer, this issue, Phys. Rev. B 27, 7301 (1983). (b) M. L. Shek, Ph.D. thesis, Stanford University, 1982 (unpublished).

[18]D. M. Kolb, R. Kötz, and K. Yamamoto, Surf. Sci. 87, 20 (1979).

[19]J. S. Hammond and N. Winograd, J. Electroanal. Chem. 80, 123 (1977); J. Electrochem. Soc. 124, 826 (1977).

[20]See S. Hüfner, G. K. Wertheim, and D. N. E. Buchanan, Solid State Commun. 14, 1173 (1974), for x-ray photoemission data.

[21]See J. Stöhr, G. Apai, P. S. Wehner, F. R. McFeely, R. S. Williams, and D. A. Shirley, Phys. Rev. B 14, 5144 (1976), for soft-x-ray photoemission data.

[22](a) G. A. Burdick, Phys. Rev. 129, 138 (1963). (b) F. M. Mueller, *ibid.* 153, 659 (1967).

[23]J. R. Smith, J. G. Gay, and F. J. Arlinghaus, Phys. Rev. B 21, 2201 (1980).

[24]D. E. Eastman and W. D. Grobman, Phys. Rev. Lett. 30, 177 (1973).

[25]G. S. Painter, Phys. Rev. B 17, 3848 (1977).

[26]B. Johansson and N. Mårtensson, Phys. Rev. B 21, 4427 (1980).

[27]G. Tréglia, M. C. Desjonqueres, D. Spanjaard, Y. Lassailly, C. Guillot, Y. Jugnet, Tran Minh Duc, and J. Lecante, J. Phys. C 14, 3463 (1981).

[28]P. Steiner, S. Hüfner, N. Mårtensson, and B. Johansson, Solid State Commun. 37, 73 (1981).

[29]P. Steiner and S. Hüfner, Solid State Commun. 37, 79 (1981).

[30]D. A. Shirley, Chem. Phys. Lett. 16, 220 (1972).

[31]A. R. Miedema, R. Boom, and F. R. De Boer, J. Less-Common Met. 41, 283 (1975).

[32]The solution energy of A in B,

$$E(A \text{ in } B)=\frac{2V_A^{2/3}(1+a\Delta\Phi^*)P}{n_A^{-1/3}+n_B^{-1/3}} \times |\Delta\Phi^*|^2+R'-9.4|(\Delta n)^{1/3}|^2 ,$$

where V_A is the atomic volume per mole of A, $\Delta\Phi^*(=\Phi_A^*-\Phi_B^*)$ is the difference in the modified work-function parameters, and n_A, n_B are the electron densities at the Wigner-Seitz cell boundaries of A and B, respectively. The values of $V^{2/3}$, Φ^*, and $n^{1/3}$ are tabulated in Ref. 31. As in Ref. 28, we use general values of $a=0.09$ and $P=0.128$. For the few systems we shall deal with in this paper, $R'=0$ except when the element A is Zn. For Zn in Cu, $R'=0.42$; for Zn in transition metals, $R'=1.42$.

[33]A. R. Miedema and J. W. F. Dorleijn, Surf. Sci. 95, 447 (1980).

[34]C. Kittel, *Introduction to Solid State Physics* (Wiley, New York, 1971), p. 96.

[35]A value of 2.55 Å is assumed for the thickness of the top surface layer. If the interlayer spacing of 1.8 Å is used, the surface contribution is less.

[36]We have tried to fit the observed pure Cu $2p_{3/2}$ signal with a bulk contribution and a surface contribution which is upward shifted. The resulting bulk core-level binding energy deviated from the observed value by no more than 0.05 eV.

[37]C. P. Flynn, J. Phys. F 10, L315 (1980).

[38]There is a change in atomic configuration in removing an atom from the solid into the vacuum. But, we note that the energy difference between $3d^{10}4s^1$ and, say, $3d^{9.6}4s^{1.4}$ due to s-d hybridization in the solid, is alreay accounted for in the cohesive energy term. The screening charge in the solid has 40% d and 60% s character, so that d^9s^2 is still a valid description for the fully screened Cu atom in the solid after ionization. The energy term for the cohesive energy of Zn serves to make the screening s charge appropriate to the s wave function around the ionized Cu atom in the solid. The effects of changes in the valence-electron hybridization on the core levels are, of course, similarly taken care of in this thermodynamical model. However, in the case of core ionization, the fully screened atom is like $3d^{10}4s^2$.

[39]C. E. Moore, *Atomic Energy Levels,* Natl. Stand. Ref. Data Ser., Natl. Bur. Stand. (U.S.), Circ. No. 35 (U.S. GPO, Washington, D.C., 1971).

[40]This value is slightly different from the value of 3.2 eV obtained in Ref. 36. We have used different energy terms for the metallic state.

[41]The following are the energy values calculated from Miedema's semiempirical approach: E(Zn in Cu)=0.3089 eV/atom, E(Cu in Pt)=0.2107 eV/atom, E(Zn in Pt)=1.347 eV/atom, E(Cu in Ni)=−0.2241 eV/atom, E(Zn in Ni)=0.6811 eV/atom, and E(Cu in Zn)=0.2817 eV/atom; E(Cu on Cu)=2.7455 eV/atom, E(Cu on Pt)=3.315 eV/atom, E(Zn on Cu)=1.5541 eV/atom, and E(Zn on Pt)=2.331 eV/atom, from Ref. 32.

[42]R. Hultgren, P. D. Desai, D. T. Hawkins, M. Gleiser, and K. K. Kelley, *Selected Values of the Thermodynamic Properties of Binary Alloys* (American Society of Metals, Metals Park, Ohio, 1973).

[43]The following are the available experimental energy values from Ref. 42 (partial molar heats of solution for solid alloys) which we use in place of the corresponding values listed in Ref. 41: E(Zn in Cu, 0% Zn)=0.2385 eV/atom, E(Cu in Pt, 0% Cu)=0.2979 eV/atom, E(Cu in Ni, 0% Cu)=−0.1214 eV/atom, and E(Cu in Zn, 15.3% Cu)=0.3917 eV/atom in ϵ phase.

[44]S. Hüfner, G. K. Wertheim, and J. H. Wernick, Phys. Rev. B 8, 4511 (1973). This value is derived by extrapolation to 0% Cu in a series of NiCu polycrystalline samples studied by x-ray photoemission. However, because the Cu peak overlaps with the bottom part of the Ni d band, it may be difficult to extract the centroid of the Cu peak. In the paper, it is not stated how this is done.

[45]J. R. Smith, F. J. Arlinghaus, and J. G. Gay, Phys Rev. B 26, 1071 (1982).

[46]G. K. Wertheim *et al.* (unpublished).

[47]P. T. Andrews and L. A. Hisscott, J. Phys. F 5, 1568 (1975). The sample is $Cu_{0.2}Zn_{0.8}$, a disordered hcp ϵ brass, and is studied by x-ray photoemission. The Cu peak shape, as judged from a given figure, is quite symmetrical. Hence, the centroid should lie at approximately the peak maximum-energy position.

[48]A. R. Williams and N. D. Lang, Phys. Rev. Lett. 40, 954 (1978).